Current Biology

Supplemental Information

Cyclin B3 Is a Mitotic Cyclin that Promotes the Metaphase-Anaphase Transition

Kai Yuan and Patrick H. O'Farrell

Supplemental Figures and Legends

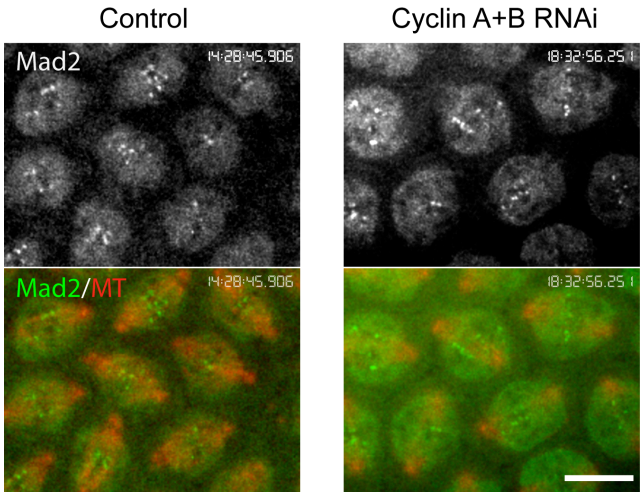

Figure S1, Kinetochore recruitment of Mad2 reveals SAC activation. Related to Figure 2. Embryos expressing GFP-Mad2 were treated with indicated cyclin RNAi. Rhodamine-labeled tubulin was injected to visualize mitotic spindles. Kinetochore localization of Mad2 was similar in control and dsRNA-injected embryos in prometaphase. Bar: 5 μm.

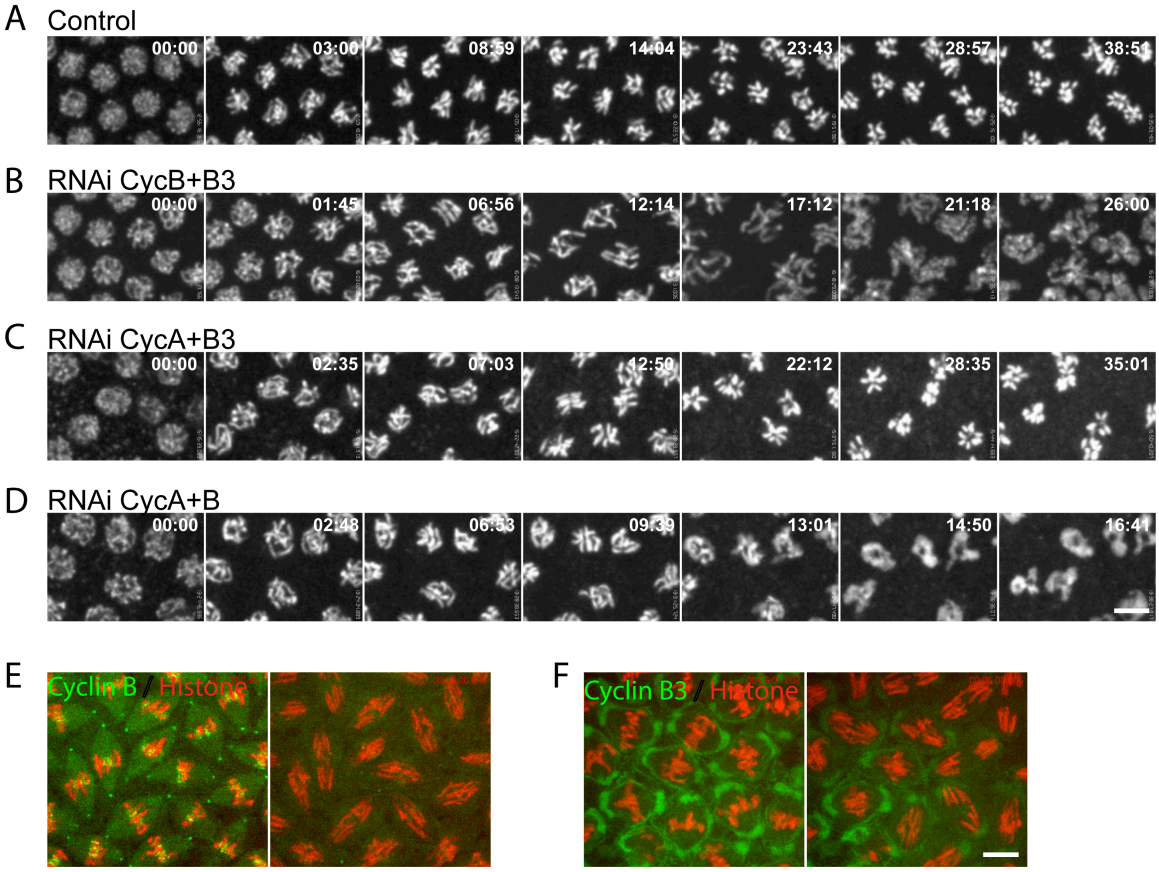

Figure S2, Cyclin-type influences the ability of SAC to arrest mitosis. Related to Figure 2.
(A-D) Control and pairwise cyclin RNAi-treated embryos were challenged with colchicine, and the behavior of mitotic chromosomes, visualized by H2AvD-GFP, was recorded. In control embryos (A) and embryos running on only Cyclin B (C), injection of microtubule poison colchicine induced robust mitotic arrests as evidenced by the persistence of chromosome condensation (38:54 in panel A, and

35:01 in panel C); while in embryos running on Cyclin A or Cyclin B3 alone, colchicine injection failed to cause similar arrests (chromosome decondensation started at 17:12 in panel B and 14:50 in panel D). Bar: 5 μm.

(E) Cyclin B-GFP protein produced from injected mRNA localized to centrosomes, kinetochores, and spindles in metaphase (left) and declined upon progress to anaphase (right).

(F) Cyclin B3-GFP was enriched on nuclear envelope/ER-like membranous structures in mitosis. Its level declined during the progress of anaphase (right). Bar: 5 μm.

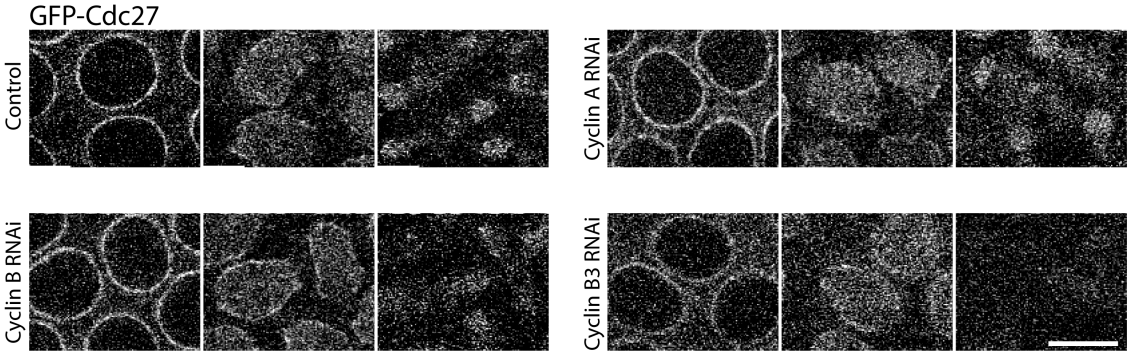

Figure S3, Anaphase chromosomal localization of Cdc27 depends on Cyclin B3. Related to Figure 3. GFP-Cdc27 was recruited to anaphase chromosomes in wild type but not Cyclin B3 RNAi-treated embryos. Note that nuclear envelope localization of Cdc27-GFP was also reduced in Cyclin B3 dsRNA injected embryos. Bar: 5 μm.

Supplemental Experimental Procedures

Fly stocks

Flies expressing either Histone H2AvD-GFP or H2AvD-RFP were used in most of the experiments [S1]. Stocks ;;pUba-GFP-Mad2 and ;;pUba-GFP-Cdc27 [S2] were used to monitor the SAC and APC/C respectively. The SAC mutants H2AvD-GFP/CyO;*mad2*^{p} and *bubR1-KEN;mad2*^{p} [S3, S4] were used to study the contribution of SAC to the timing of metaphase-anaphase transition in the early embryos. The *cycB3* mutant (Bloomington stock No. 6635) was either homozygosed or trans-heterozygosed over a deficiency (Bloomington stock No. 7679) to characterize the female sterility. A stock H2AvD-RFP/CyO;*cycB3*/TM6,*Tb* was created to study the neuroblast divisions.

Reagents used in microinjections

The production and use of double-stranded RNA (dsRNA) targeting mitotic cyclins were described previously [S5]. The production of mRNA of the three mitotic cyclins was detailed in our previous paper [S6]. The mRNA was used at the concentration of 600 ng/μL. UbcH10^{C114S} (a gift from K. Nasmyth, University of Oxford, Oxford, UK) was made and used as previously described [S7]. GST-Cyclin B (a gift from W. Sullivan, University of California, Santa Cruz, CA) was injected at the concentration of 31 μM. His-tag stable Cyclin B (CycB^{S}, Δ-46) [S8] was purified and used at the concentration of 15 μM. Colchicine was injected at 1 mg/mL. Rhodamine-labeled tubulin protein was purchased from Cytoskeleton (Denver, CO). Oregon green conjugated wheat germ agglutinin (WGA) was purchased from Molecular Probes (Eugene, OR).

Microinjection, imaging and data interpretation

In all the experiments, the dsRNA was injected around the 9th nuclear division. We have previously shown that injection of dsRNA complementary to all three mitotic cyclins at this stage arrested embryos in interphase 12 or 13 [S5], indicating that this time course gives sufficient time for RNAi knockdown of targeted cyclins. In addition, it is noteworthy that we have characterized the phenotypes of the different cyclin knockdowns at different doses of dsRNA and at different times and that the distinctive phenotypes associated with the different cyclin types are evident at all points during the knockdown [S5, S9]. Furthermore, studies that incorporate other modes of changing cyclin levels, whether it is mutation, reduction of gene dose, transgenes expression, injection of cyclin proteins, or expression of injected cyclin mRNA, all suggest that each cyclin makes distinctive contributions not compensated by the level of other cyclins [S8-S12]. The lack of distinctive effects due to changes in level as opposed to changes in distribution of cyclin types means that the analysis we report here is not dependent on a complete knockdown, and only requires an effective knockdown.

The mRNA was injected into pre-blastoderm embryos shortly after egg laying. Colchicine, rhodamine-labeled tubulin, Oregon green-labeled WGA, and other recombinant proteins were injected before filming.

Embryos were collected and treated as previously described [S6], covered with halocarbon oil, and imaged with a spinning-disk confocal system (CSU10; Yokagowa) equipped on an inverted Leica DM IRB microscope with a 100X plan Fluotar 1.3 NA objective. Images were collected at 1 μm over a 5 μm range using a controlled stage (MS-2000; Applied Scientific Instrumentation). All images were captured and analyzed in Volocity 6 (PerkinElmer). Statistical analysis was done in Prism (GraphPad Software).

For immuno-staining of defective embryos from *cycB3* females, eggs from a 2-hour collection were fixed in methanol, and stained with a mixture of 1:50 each anti-tubulin AA12.1, AA4.3, and E7 mouse monoclonals (Developmental Studies Hybridoma Bank) overnight. DNA was visualized by a 15 min staining with 1:500 PicoGreen (Molecular Probes).

For live imaging of neuroblast divisions, third instar larval brains were dissected and processed as previously described [S4]. Images were collected at 1 μm over a 5 μm range, and metaphase duration was determined by analyzing mitotic chromosomes visualized by H2AvD-RFP.

References

S1. Clarkson, M., and Saint, R. (1999). A His2AvDGFP fusion gene complements a lethal His2AvD mutant allele and provides an in vivo marker for Drosophila chromosome behavior. DNA and cell biology *18*, 457-462.

S2. Huang, J.Y., and Raff, J.W. (2002). The dynamic localisation of the Drosophila APC/C: evidence for the existence of multiple complexes that perform distinct functions and are differentially localised. Journal of cell science *115*, 2847-2856.

S3. Buffin, E., Emre, D., and Karess, R.E. (2007). Flies without a spindle checkpoint. Nature cell biology *9*, 565-572.

S4. Rahmani, Z., Gagou, M.E., Lefebvre, C., Emre, D., and Karess, R.E. (2009). Separating the spindle, checkpoint, and timer functions of BubR1. The Journal of cell biology *187*, 597-605.

S5. McCleland, M.L., and O'Farrell, P.H. (2008). RNAi of mitotic cyclins in Drosophila uncouples the nuclear and centrosome cycle. Current biology : CB *18*, 245-254.

S6. Farrell, J.A., Shermoen, A.W., Yuan, K., and O'Farrell, P.H. (2012). Embryonic onset of late replication requires Cdc25 down-regulation. Genes Dev *26*, 714-725.

S7. Oliveira, R.A., Hamilton, R.S., Pauli, A., Davis, I., and Nasmyth, K. (2010). Cohesin cleavage and Cdk inhibition trigger formation of daughter nuclei. Nature cell biology *12*, 185-192.

S8. Parry, D.H., and O'Farrell, P.H. (2001). The schedule of destruction of three mitotic cyclins can dictate the timing of events during exit from mitosis. Current biology : CB *11*, 671-683.

S9. McCleland, M.L., Farrell, J.A., and O'Farrell, P.H. (2009). Influence of cyclin type and dose on mitotic entry and progression in the early Drosophila embryo. The Journal of cell biology *184*, 639-646.

S10. Sigrist, S., Jacobs, H., Stratmann, R., and Lehner, C.F. (1995). Exit from mitosis is regulated by Drosophila fizzy and the sequential destruction of cyclins A, B and B3. The EMBO journal *14*, 4827-4838.

S11. Lehner, C.F., and O'Farrell, P.H. (1990). The roles of Drosophila cyclins A and B in mitotic control. Cell *61*, 535-547.

S12. Yuan, K., Farrell, J.A., and O'Farrell, P.H. (2012). Different cyclin types collaborate to reverse the S-phase checkpoint and permit prompt mitosis. Journal of Cell Biology *198*, 973-980.